PLOS ONE

RESEARCH ARTICLE

Mild phenotype of knockouts of the major apurinic/apyrimidinic endonuclease APEX1 in a non-cancer human cell line

Daria V. Kim[1,2], Liliya M. Kulishova[2], Natalia A. Torgasheva[2], Vasily S. Melentyev[1,3], Grigory L. Dianov[1,3,4], Sergey P. Medvedev[3], Suren M. Zakian[3], Dmitry O. Zharkov[1,2]*

1 Department of Natural Sciences, Novosibirsk State University, Novosibirsk, Russia, 2 SB RAS Institute of Chemical Biology and Fundamental Medicine, Novosibirsk, Russia, 3 SB RAS Institute of Cytology and Genetics, Novosibirsk, Russia, 4 Department of Oncology, MRC Oxford Institute for Radiation Oncology, University of Oxford, Oxford, United Kingdom

* dzharkov@niboch.nsc.ru

Abstract

The major human apurinic/apyrimidinic (AP) site endonuclease, APEX1, is a central player in the base excision DNA repair (BER) pathway and has a role in the regulation of DNA binding by transcription factors. In vertebrates, APEX1 knockouts are embryonic lethal, and only a handful of knockout cell lines are known. To facilitate studies of multiple functions of this protein in human cells, we have used the CRISPR/Cas9 system to knock out the *APEX1* gene in a widely used non-cancer hypotriploid HEK 293FT cell line. Two stable knockout lines were obtained, one carrying two single-base deletion alleles and one single-base insertion allele in exon 3, another homozygous in the single-base insertion allele. Both mutations cause a frameshift that leads to premature translation termination before the start of the protein's catalytic domain. Both cell lines totally lacked the APEX1 protein and AP site-cleaving activity, and showed significantly lower levels of the *APEX1* transcript. The APEX1-null cells were unable to support BER on uracil- or AP site-containing substrates. Phenotypically, they showed a moderately increased sensitivity to methyl methanesulfonate (MMS; ~2-fold lower EC_{50} compared with wild-type cells), and their background level of natural AP sites detected by the aldehyde-reactive probe was elevated ~1.5–2-fold. However, the knockout lines retained a nearly wild-type sensitivity to oxidizing agents hydrogen peroxide and potassium bromate. Interestingly, despite the increased MMS cytotoxicity, we observed no additional increase in AP sites in knockout cells upon MMS treatment, which could indicate their conversion into more toxic products in the absence of repair. Overall, the relatively mild cell phenotype in the absence of APEX1-dependent BER suggests that mammalian cells possess mechanisms of tolerance or alternative repair of AP sites. The knockout derivatives of the extensively characterized HEK 293FT cell line may provide a valuable tool for studies of APEX1 in DNA repair and beyond.

Introduction

Many endogenous and environmental factors generate a steady stream of lesions in cellular DNA. Estimates based on known rates of spontaneous DNA damage suggest that ~20,000 endogenous lesions appear in each cell's DNA per day [1]. Base excision repair (BER) is the system primarily responsible for the removal of small non-bulky lesions from DNA [2, 3]. BER is initiated by various DNA glycosylases, each of which is specific to a characteristic type of damage. DNA glycosylases recognize damaged bases and hydrolyze their *N*-glycosidic bonds, leaving a baseless deoxyribose residue (apurinic/apyrimidinic site, or AP site). The AP site is further processed by an AP endonuclease (APEX1 in mammals), which cleaves the phospho-diester bond 5′ to the lesion. DNA polymerase β (POLβ) then eliminates the blocking 2′-deoxyribose-5′-phosphate and inserts an undamaged dNMP. At the final stage, the complex of XRCC1 adaptor protein and DNA ligase IIIα seals the remaining nick.

Besides being an intermediate in BER, AP sites are among the most abundant spontaneously arising DNA lesions [4–6]. AP sites are non-instructional and thus strongly mutagenic, often directing dAMP misincorporation [7, 8]. In addition, AP sites are toxic for cells via multiple mechanisms, including DNA strand breakage, transcription errors, and covalent trapping of DNA-bound proteins such as histones and topoisomerases [9–12]. In yeast, a full depletion of the AP site repair capability is lethal [13]. *E. coli* cells devoid of AP site-processing activities are exceedingly sensitive to a variety of genotoxic agents and chronically induces the SOS response, indicating persisting DNA damage [14–16].

APEX1 (also known as APE1, HAP1, or Ref-1) is one of the key BER elements involved in the repair of AP sites in human cells [17–20]. In addition to its endonuclease activity, APEX1 exhibits redox activity directed to several transcription factors, such as AP-1 (Jun/Fos), NF-κB, HIF-1a, CREB, and p53 [18, 19, 21, 22], reducing oxidized cysteines in the DNA-binding domains of these proteins and thereby stimulating their ability to bind DNA. Recently, APEX1 was shown to play a role in RNA processing and quality control [23, 24].

To elucidate the effect of AP sites and the role of APEX1 at the cell and organism level, several attempts have been made to obtain knockout mice and cell lines. However, $Apex1^{-/-}$ mouse embryos die at the early stages of development and failed to produce cell lines [25–28]. Embryonic fibroblasts can be isolated from transgenic mice with the floxed human *APEX1* gene but enter apoptosis after the induction of the cassette removal [28]. In zebrafish embryos, morpholino knockdown of *apex1* is lethal due to abnormal formation of the early cardiovascular system [29]. On the other hand, $Apex1^{+/-}$ mice are viable and fertile but tumor-prone and hypersensitive to oxidative stress [27, 30, 31].

Presently, there are few mammalian cell models with stably inactivated genes encoding APEX1 homologs [32]. A knockout was generated by a conventional recombination approach in the hypotriploid mouse B-cell line CH12F3, producing cells hypersensitive to MMS [33]. Also, a CRISPR/Cas9 knockout derivative of breast cancer HCC1937 cell line was reported [34]. However, the majority of studies on the functional deficiency of APEX1 in mammalian cells so far involved downregulation of *APEX1* expression. Knockdown of *APEX1* sensitizes cells to a wide range of genotoxic assaults, such as ionizing radiation, oxidative stress (H$_2$O$_2$, paraquat, bleomycin), alkylating agents (methyl methanesulfonate (MMS), temozolomide, thiotepa), crosslinkers, and topoisomerase inhibitors [35–38]. Although the knockdown models proved very useful, to follow the effects of the full lack of APEX1 in the long term it would be desirable to have an APEX1-deficient derivative of a well-characterized cell line. Here we report the generation and characterization of a CRISPR/Cas9 *APEX1* knockout in the extensively studied non-cancer HEK 293FT human cell line. Although these cells were not able to complete BER at the biochemical level and demonstrated an increased level of AP sites, the

phenotypic consequences were surprisingly mild, suggesting the existence of AP sites tolerance or alternative repair pathways in mammalian cells.

Materials and methods

Cells, plasmids, oligonucleotides and enzymes

HEK 293FT cell line was from Thermo Fisher Scientific (Waltham, MA; Cat. #R70007). The supported laboratory stock was checked by PCR for the absence of mycoplasma contamination. Plasmid pSpCas9(BB)-2A-GFP (PX458; [39]) was a gift from Feng Zhang (Addgene plasmid #48138; http://n2t.net/addgene:48138; RRID: Addgene_48138). Restriction endonucleases AsiGI, DraIII, PctI, proteinase K, and *E. coli* uracil–DNA glycosylase (Ung) were purchased from Sibenzyme (Novosibirsk, Russia), restriction endonuclease BbsI and phage T4 DNA ligase were from New England Biolabs (Beverly, MA), and *Taq* DNA polymerase, from Thermo Fisher Scientific (Waltham, MA). Recombinant human APEX1 was purified as described [40]. Recombinant rat DNA POLβ, purified as described [41], was a kind gift from Dr. Nina Moor (SB RAS ICBFM). Polyclonal rabbit anti-APEX1 antibodies raised against the full-length affinity-purified protein (NB100-101) were from Novus Biologicals (Centennial, CO), and secondary goat anti-rabbit antibodies (ab6791) were from Abcam (Cambridge, UK). The oligonucleotides used in this study are listed in S1 Table. The oligonucleotides, including modified ones, were synthesized at the SB RAS ICBFM oligonucleotide synthesis facility and gel-purified before use.

Generation of knockout lines

Inserts corresponding to the designed sgRNA were cloned into the BbsI site of pX458. This plasmid carries a constitutively expressed *Streptococcus pyogenes* Cas9 gene linked to the eGFP reporter through a T2A ribosome skipping sequence, and a cassette for U6 promoter-driven sgRNA synthesis [39]. The plasmids were purified from *E. coli* DH5α using a Plasmid Mini Kit (Qiagen, Venlo, Netherlands), and the correctness of the insert was confirmed by Sanger sequencing. HEK 293FT cells (~10^5 cells) were transfected with 1.25 μg of the plasmid using Lipofectamine 3000 (Thermo Fisher Scientific). After 48 h, ~1000 GFP-positive cells were collected using S3e Cell Sorter (Bio-Rad Laboratories, Hercules, CA), diluted into 96-well plates at 0.5, 1, and 2 cells per well, and grown as described [39]. The wells containing microscopically observed monoclones were allowed to grow until ~60% monolayer density, after which half of the cells were separated and frozen to maintain the clone. The other half was grown to a 100% monolayer, trypsinized and analyzed. Genomic DNA was obtained by lysis in the buffer containing 10 mM Tris–HCl (pH 8.0), 10 mM EDTA, 3.5% Igepal CA630, 3.5% Tween 20, and 0.4 mg/ml Proteinase K for 3 h at 65˚C followed by phenol–chloroform extraction. For tracking of indels by decomposition (TIDE) analysis, the genomic DNA was PCR-amplified, purified with QIAquick PCR Purification Kit (Qiagen) and subjected to Sanger sequencing. For genotyping, the PCR products were digested with DraIII for 1 h at 37˚C. For sequencing individual alleles, the PCR products were subcloned into the pCR2.1 vector using TA Cloning Kit (Thermo Fisher Scientific).

Real-time RT-PCR

Total RNA was purified using RNeasy Plus Mini Kit (Qiagen). Reverse transcription from a (dT)$_{16}$ primer and 1 μg RNA was done with M-MuLV–RH First Strand cDNA Synthesis Kit (Biolabmix, Novosibirsk, Russia) according to the manufacturer's instructions. PCR was performed on a LightCycler 96 instrument (Roche Applied Science, Penzberg, Germany) using a

BioMaster HS-qPCR SYBR Blue kit (Biolabmix). The sequences of the primers are given in S1 Table; all primer pairs were designed to anneal within sequences from different exons or to span an exon/exon border in cDNA. β2-Microglobulin was used as a reference gene to normalize the target gene expression [42]. Two biological replicates were performed, for each one 1–3 independent cDNA preparations were made on different days, each preparation was analyzed in triplicate.

Enzyme activity in cell extracts

Whole-cell extracts were prepared according to [43]. In the assay for AP endonuclease activity, the reaction mixture (10 μl) included 20 mM Tris–HCl (pH 8.0), 50 mM NaCl, 10 mM $MgCl_2$, 2 mM dithiothreitol (DTT), 5% glycerol, 40 ng of the cell extract, and 50 nM 23-mer 5′-fluorescein-labeled duplex substrate containing a (3-hydroxytetrahydrofuran-2-yl)methyl phosphate residue (THF). The reaction was allowed to proceed for 10 min at 37˚C and terminated by adding 5 μl of deionized formamide and heating for 5 min at 95˚C. The reaction products were analyzed by electrophoresis in 20% polyacrylamide gel containing 8 M urea and visualized using a Typhoon FLA 9500 Imager (GE Healthcare, Chicago, IL). In the assay for uracil–DNA glycosylase activity, the substrate contained dU instead of THF, and the reaction was stopped by adding NaOH to 0.1 M and heating for 2 min at 95˚C. The mixture was neutralized by equimolar HCl and processed as above. In the gap-filling assay, the substrate consisted of an 11-mer primer, 40-mer template, and a 28-mer downstream strand (S1 Table), which upon assembly produced a single-nucleotide gap with T in the template. The reaction was performed in 50 mM Tris–HCl (pH 7.5), 10 mM $MgCl_2$, 10 mM DTT, 0.1 mM dATP, supplemented with 50 nM substrate and 1 μg cell extract for 30 min at 37˚C and processed as indicated above for the AP endonuclease reaction.

DNA repair assay

The reaction mixture (10 μl) included 50 nM 5′-^{32}P-labeled THF:C or U:C substrate and 1 μg cell extract in BER buffer containing 50 mM Tris–HCl (pH 7.5), 10 mM $MgCl_2$, 10 mM DTT, 0.1 mM dGTP, and 1 mM ATP, or in POLβ buffer containing 10 mM Tris–HCl (pH 7.6), 10 mM $MgCl_2$, 1 mM DTT, and 0.1 mM dGTP. The reaction was allowed to proceed for 30 min at 37˚C and terminated by adding 5 μl of formamide dye (20 mM EDTA, 0.1% xylene cyanol, 0.1% bromophenol blue in formamide) and heating for 5 min at 95˚C. In the case of the U:C substrate, some of the completed reactions were treated with 100 nM *E. coli* Fpg protein for 5 min at 37˚C to confirm that the AP site was present, and then terminated as above. The reaction products were analyzed by electrophoresis in 20% polyacrylamide gel containing 8 M urea and visualized using a Typhoon FLA 9500 Imager.

Doubling time experiments

Cells were grown in Dulbecco's modified Eagle's medium supplemented with 10% fetal bovine serum, 100 U/ml penicillin, 100 U/ml streptomycin, and 0.25 μg/ml amphotericin B at 37˚C under 5% CO_2. Exponentially growing cells were seeded in 24-well plates at 4×10^4/well. Each 24 h the cells were trypsinized and counted using a Luna II automated cell counter (Logos Biosystems, South Korea).

Cell cycle experiments

Exponentially growing cells were seeded in 6-well plates at 10^4/well. Twenty-four hours later the cells were collected in cold PBS and counted. One million cells were fixed in 70% ethanol

at 4˚C for 24 h, washed in PBS and stained in 1 ml of the solution containing 0.1% (v/v) Triton X-100, 20 μg of propidium iodide, 200 μg of DNase-free RNase A for 15 min at 37˚C. Immediately after staining, the cells were analyzed using NovoCyte 3000 flow cytometer (Agilent Technologies, Santa Clara, CA); PE Texas Red channel was used to detect the propidium iodide signal.

Cell viability

The cell viability was determined using 3-(4,5-dimethylthiazol-2-yl)-2,5-diphenyltetrazolium bromide (MTT). Solutions of H_2O_2, $KBrO_3$, and MMS were prepared in serum-free medium. Cells were seeded in 96-well plates at 4.5×10^3/well. After 24 h, an equal volume of chemical-containing medium was added to the cells for 24 h (H_2O_2) or 48 h ($KBrO_3$ and MMS). After the incubation, the growing media was removed, and 0.25 mg/ml MTT solution in the medium was added for 2 h. Then the MTT-containing medium was aspirated, and formazan crystals were dissolved in DMSO. The optical density was measured at 570 nm and 620 nm using Apollo-8 Microplate Absorbance Reader LB 912 (Berthold Technologies, Bad Wildbad, Germany). The cell viability was calculated as the percentage of staining intensity in treated wells relative to the control.

Aldehyde reactive probe assay

The levels of AP sites were determined using the DNA damage assay kit (ab211154, Abcam, Cambridge, UK) according to the manufacturer's protocol. Cells were seeded in 6-well plates at 3×10^5/well. After 24 h, the cells were briefly rinsed in phosphate-buffered saline (PBS) and incubated for 1 h in 1 mM MMS dissolved in dimethyl sulfoxide (DMSO); as a control, 0.1% DMSO solution in PBS was used. Then the cells were again rinsed in PBS and incubated for 2 hours in the complete medium. After that, the cells were collected by trypsinization, washed in PBS, and the genomic DNA was extracted using QIAamp DNA mini kit (Qiagen) and used for AP site determination.

Results

APEX1 gene knockout in HEK 293FT cells

Using the on-target and off-target effect estimator implemented in the benchling.com platform [44, 45], we have designed three sgRNA sequences targeting protospacers in the human *APEX1* gene, aiming to introduce a frameshift mutation near the beginning of the coding sequence where it would more likely to inactivate the protein product (Fig 1A, S1 Fig). Two of the protospacers were located in exon 2 spanning the initiator ATG codon and were shifted by a single base relative to each other, leading to the use of different protospacer-adjacent motif (PAM) sequences: TGG for Protospacer 1 and GGG for Protospacer 2. The third protospacer was fully located in the coding part of the gene (exon 3).

After the plasmid transfection and sorting of GFP-positive cells, we have amplified the target genomic region by PCR and used tracking of indels by decomposition (TIDE) approach to compare the efficiency of the sgRNA in inducing frameshift mutations [46]. Overall, ~17% of the PCR products carried an insertion or a deletion in all three cases (Fig 1B). However, the products of transfection with a plasmid producing sgRNA targeting Protospacer 3 were mostly single-base deletions or insertions, whereas the other two sgRNAs induced a more diverse range of indels (Fig 1B). Since ±1 indels unambiguously produce a frameshift, we went forward with the cell population resulting from Cas9 targeting by sgRNA #3.
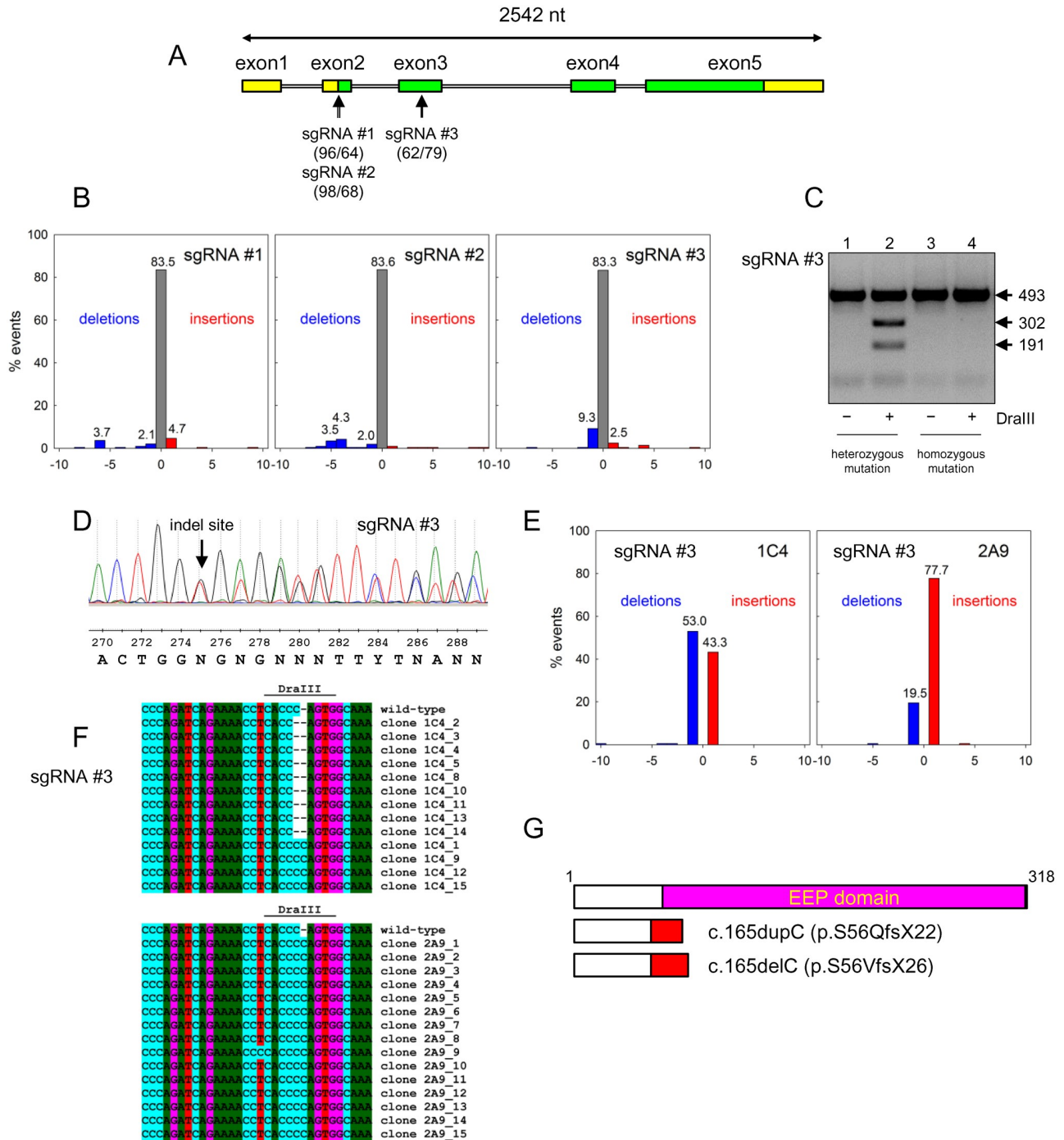
Fig 1. Generation of APEX1 knockout cells using CRISPR/Cas9 technology. A, map of human APEX1 gene and location of the protospacers targeted by sgRNAs. Numbers in parentheses correspond to efficiency and specificity scores calculated by benchling.com; higher scores indicate better efficiency and better specificity. Green parts of the exons correspond to the protein-coding sequence. **B,** TIDE analysis of the distribution of mutation events in the pool of HEK 293FT cells after transfection with pX458 expressing different sgRNAs. The blue bars represent deletions, the red bars, insertions, the grey bars, sequences with no mutations. The X axis shows the distance from the target cleavage site in nucleotides. **C,** cleavage of the PCR-amplified part of the *APEX1* gene by DraIII in wild-type cells (*lanes 1, 2*) and after a successful knockout induced by sgRNA#3 (*lanes 3, 4*). Arrows mark the mobility of the full-length PCR product (493 nt) and the cleavage fragments. **D,** representative capillary sequencing chromatogram (ABI 3130xl instrument; complementary strand sequenced) of the PCR-amplified part of the *APEX1* gene from the DraIII-negative clone 1C4. **E,** TIDE analysis of the distribution of mutation events in 1C4 and 2A9 single cell clones induced by sgRNA#3. **F,** sequences of the protospacer region in subcloned fragments from 1C4 and 2A9 cells. **G,** truncated APEX1 proteins arising from the single-base insertion and single-base deletion at nucleotide 165. Changed polypeptide parts after the frameshift are colored red. The catalytic EEP domain is shown in magenta.

Of 113 obtained monoclones after transfection with pX458 expressing sgRNA#3, we have genotyped 19 random clones using DraIII restriction endonuclease, the site of which (5′-CACNNNGTG-3′) overlaps the 3′-terminus of the protospacer (Fig 1C, S1 Fig). Six of the clones had lost all copies of the DraIII site; two of the clones (1C4 and 2A9) were randomly selected and analyzed by TIDE (Fig 1D and 1E, S2 Fig). In both clones, more than 97% PCR products carried a mutation. In 1C4, we have observed an approximately equal ratio of single-base insertions and deletions (~1.2-fold more deletions), whereas the 2A9 clone carried ~4-fold more +1 insertions than −1 deletions (Fig 1E). To characterize the genotype of the clones more precisely, we have subcloned the PCR products and sequenced 13 clones for 1C4 and 15 clones for 2A9 (Fig 1F). Four of the 1C4 clones carried an insertion of C within the DraIII site (c.165dupC), whereas nine carried a deletion of C within this site (c.165delC). All 2A9 clones carried the c.165dupC insertion, and one of the clones had an additional T>C substitution immediately before the DraIII site (c.160T>C). Since HEK 293FT is a hypotriploid cell line and carries three copies of the 14q11.2 chromosomal region where the *APEX1* gene is located, we conclude that the most likely genotype of 1C4 cells is two c.165delC alleles and one c.165dupC allele, whereas 2A9 carries three c.165dupC alleles, one of which possibly carries a c.160T>C mutation. The presence of this substitution might be a source of erroneous decomposition as a deletion allele by TIDE. Given the number of sequenced subclones, the probability of missing a wild-type allele in monoclones of hypotriploid cells would be $\sim 5 \times 10^{-3}$ for 1C4 and $\sim 2 \times 10^{-3}$ for 2A9.

At the polypeptide level, the c.165dupC variant retains the first 55 amino acid residues of the wild-type protein, and, after the frameshift, produces a stop codon, terminating after residue 76 (p.S56QfsX22). The c.165delC variant retains the same first 55 amino acid residues and produces a stop codon after residue 80 (p.S56VfsX26). Both mutations completely eliminate the catalytic domain of the APEX1 protein as well as the Cys65 residue critical for its redox function (Fig 1G, S3 Fig).

APEX1 knockout cells lack functional base excision repair

To evaluate the consequences of APEX1 deletion in HEK 293FT cells, we have looked at the production of the protein by Western blotting (Fig 2A). Both 1C4 and 2A9 cells lacked the band detectable by anti-APEX1 antibodies, which was clearly seen in wild-type cells. The *APEX1* mRNA level was ~13-fold lower in 1C4 cells and 4-fold lower in 2A9 cells relative to wild-type HEK 293FT, suggesting that the mutant mRNAs undergo nonsense-mediated RNA decay (Fig 2B). In comparison, the levels of mRNA of several DNA glycosylase genes were unaffected or even elevated (Fig 2B, S4 Fig). Notably, we observed a statistically significant increase in *OGG1* mRNA in both knockout lines, whereas *MUTYH* expression was enhanced in 1C4 cells, and *NEIL2* expression, in 2A9 cells (Fig 2B). This may suggest that permanent loss of APEX1 induces a compensatory increase in DNA glycosylases that have an AP lyase activity, or those that participate in the repair of oxidative DNA damage.

We then inquired whether *APEX1* knockout is sufficient to eliminate AP site cleavage activity from the cells. Wild-type cell extracts efficiently cleaved double-stranded oligonucleotides containing an aldehydic AP site or its non-aldehydic analog, (3-hydroxytetrahydrofuran-2-yl) methyl phosphate (THF) (Fig 2C, lanes 3 and 8). However, no cleavage products were observed in the extracts of the knockout cell lines (Fig 2C, lanes 4–5 and 9–10). At the same time, both wild-type and *APEX1*-null cells were fully proficient in the ability to excise uracil from DNA (S5A Fig) and to incorporate a dNMP into a gapped DNA substrate (S5B Fig). This indicates that the BER pathway is functional in the knockout cells both upstream (base removal) and downstream (gap filling) of the AP endonuclease step.
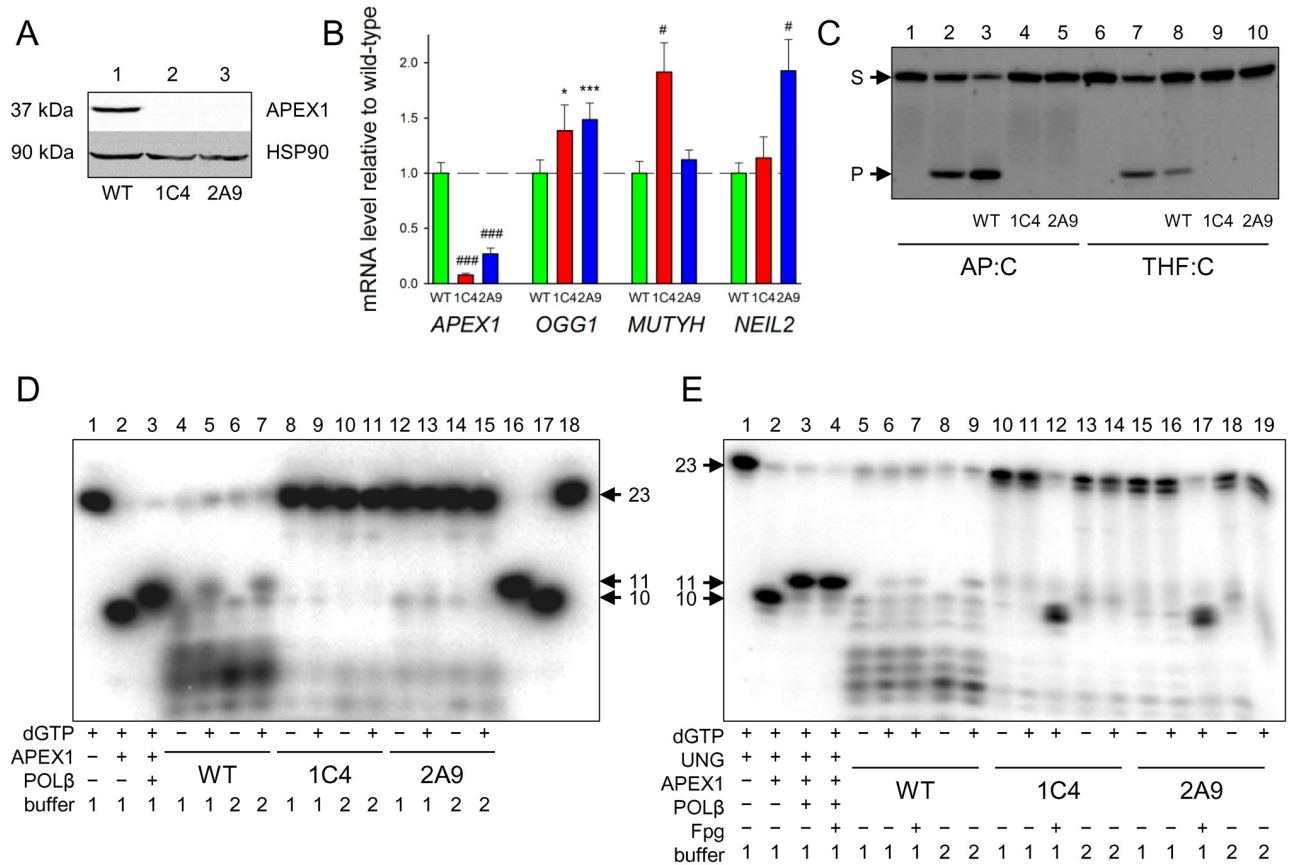
Fig 2. APEX1 knockout cells lack detectable APEX1 protein, AP endonuclease activity, and BER. A, Western blot for APEX1 in the extracts of wild-type HEK 293 (*lane 1*) and knockout cells 1C4 (*lane 2*) and 2A9 (*lane 3*). **B,** mRNA levels of *APEX1*, *OGG1*, *MUTYH*, and *NEIL2* genes in 1C4 and 2A9 cells relative to wild-type HEK 293FT. Mean ± s.d. are shown (*n* = 4, see Materials and methods for a detailed description). Student's unpaired *t* test: *, $p < 0.05$; ***, $p < 0.005$; #, $p < 0.001$; ###, $p < 0.0001$. **C,** cleavage of a 23-mer duplex oligonucleotides containing an AP:C pair (*lanes 1–5*) or a THF:C pair (*lanes 6–10*) by extracts of wild-type HEK 293 (*lanes 3 and 8*) and knockout cells 1C4 (*lanes 4 and 9*) and 2A9 (*lanes 5 and 10*). *Lanes 1 and 6*, no enzyme or cell extract; *lanes 2 and 7*, recombinant APEX1. Arrows mark the mobility of the substrate (S) and the cleavage product (P). **D,** repair of a THF:C duplex. *Lanes 1–3*, repair system reconstituted from purified APEX1 and POLβ, as indicated below the gel. *Lanes 4–7*, extracts of wild-type HEK 293; *lanes 8–11*, extracts of 1C4 cells; *lanes 12–15*, extracts of 2A9 cells. Buffer 1, BER buffer, buffer 2, POLβ buffer (see Materials and methods). *Lanes 16–18*, size markers, as specified by the arrows. **E,** repair of a U:C duplex. *Lanes 1–4*, repair system reconstituted from purified UNG, APEX1 and POLβ, as indicated below the gel. *Lanes 5–9*, extracts of wild-type HEK 293; *lanes 10–14*, extracts of 1C4 cells; *lanes 15–19*, extracts of 2A9 cells. Buffers are as in *Panel D*. Some reactions were post-treated by Fpg to confirm the AP site formation. C–E, representative gels from 3–4 experiments.

To evaluate the BER proficiency of the knockout cells, we have treated duplexes containing either U or THF residues with the cell extracts in the presence of dNTPs. In the wild-type cell extracts, we observed substrate cleavage followed by strong $3' \rightarrow 5'$ exonucleolytic degradation, which may be ascribed to either APEX1 itself or other exonucleases present in the extract. Interestingly, such degradation was not apparent in a gapped substrate in the polymerase experiments (S5B Fig), suggesting a requirement for an assembly of a full BER complex. Despite the exonuclease degradation, insertion of a dNTP after APEX1 cleavage was evident by the appearance of the 11-mer product (Fig 2D, lanes 5 and 7, Fig 2E, lanes 6, 7, and 9). In an attempt to enhance the accumulation of the 11-mer, we have used the reaction mixture optimal for POLβ-catalyzed gap filling [47], yet essentially the same results were observed as in the BER buffer (compare lanes 4–5 and 6–7 in Fig 2D and 5–6 and 8–9 in Fig 2E). Contrary to the wild-type extracts, only minor substrate cleavage was observed in both knockout lines, even though uracil was efficiently removed, as evidenced by the efficient cleavage of the

reaction product by Fpg, a DNA glycosylase with a strong AP lyase activity (Fig 2D, lanes 8–15, Fig 2E, lanes 10–19). Cleavage products present in trace amounts in the reactions with the U:C substrate have lower mobility than the APEX1 product and likely reflect β-elimination of aldehydic AP sites by any of AP lyases present in the cell, which generate 3′-unsaturated aldehydes that cannot be extended by DNA polymerases (S6 Fig).

Biological consequences of *APEX1* knockout

Having confirmed that the *APEX1* knockout lines are unable to support BER at the biochemical level, we set out to explore how this deficiency is manifested in the cells' phenotype. The mutant cells showed no obvious deviations in the overall cell morphology. Wild type and knockout cells showed no significant difference in population doubling time (21.7 h HEK 293FT, 20.4 h 1C4, 19.4 h 2A9, Fig 3A) or in the percentage of cells at different cell cycle stages (Fig 3B).

Knockout of *APEX1* would be expected to increase the abundance of background AP sites in the genomic DNA. To see if this is indeed the case, we have quantified the AP sites using the aldehyde-reactive probe (ARP) assay, which is based on the specific condensation of alkoxyamines with the open form of AP sites [48]. Knockout of *APEX1* led to a ~1.5–2-fold increase in the number of AP sites, comparable with the increase seen in wild-type cells in the presence of MMS (Fig 3C, S7 Fig). Interestingly, when the knockout cells were treated by MMS, we observed no additional increase in the AP sites abundance (Fig 3C). The expression of *MPG* in the *APEX1* null lines tended to be lower but this decrease did not reach statistical significance (S4 Fig), so it is unlikely that extra AP sites do not appear due to the lack of adduct excision by the glycosylase. BER-induced breaks at AP sites are believed to be the main MMS-induced cytotoxic lesions [49], so it is possible that in the absence of APEX1 the reactive aldehydic AP sites are channeled into more deleterious lesions undetectable by ARP, such as DNA–protein cross-links or oxidized AP sites [50, 51].

DNA repair-deficient cells are often characterized by increased sensitivity to various genotoxic agents. We assayed the viability of *APEX1* null lines in the presence of a range of concentrations of hydrogen peroxide, potassium bromate, and methyl methanesulfonate. H_2O_2 produces a wide range of lesions in DNA, including single-strand breaks and many oxidized bases [52, 53]. $KBrO_3$ predominantly produces 8-oxoguanine and strand breaks in a glutathione-dependent manner [54, 55]. In contrast, MMS mostly methylates guanines at N7 and adenines at N3 [56]. The resulting ring-alkylated purines are quickly converted to AP sites either by methylpurine–DNA glycosylase MPG or by spontaneous hydrolysis [49, 57, 58]. Both 1C4 and 2A9 cell lines demonstrated moderately enhanced sensitivity to MMS compared with the parent HEK 293FT cells (Fig 3D; EC_{50} ~250 μM for wild-type cells and ~120 μM for both 1C4 and 2A9). However, as can be seen in Fig 3E and 3F, no significant difference was found with respect to the sensitivity of all three cell lines to H_2O_2 and $KBrO_3$, except for 2A9 cells a 100 μM H_2O_2 ($p < 0.05$ from both wild-type and 1C4 cells), indicating the existence of backup repair pathways for cytotoxic lesions produced by these agents in addition to APEX1-dependent BER.

Discussion

APEX1 is the first common enzyme in the human BER pathway, required for the repair of all small non-bulky damaged bases and AP sites. While many bacteria have two AP endonucleases of unrelated structure but with overlapping enzyme activities (Xth and Nfo in *E. coli*), APEX1 seems to be the major human AP endonuclease supporting most of BER and carrying out additional functions such as stimulation of transcription factors binding to DNA, RNA
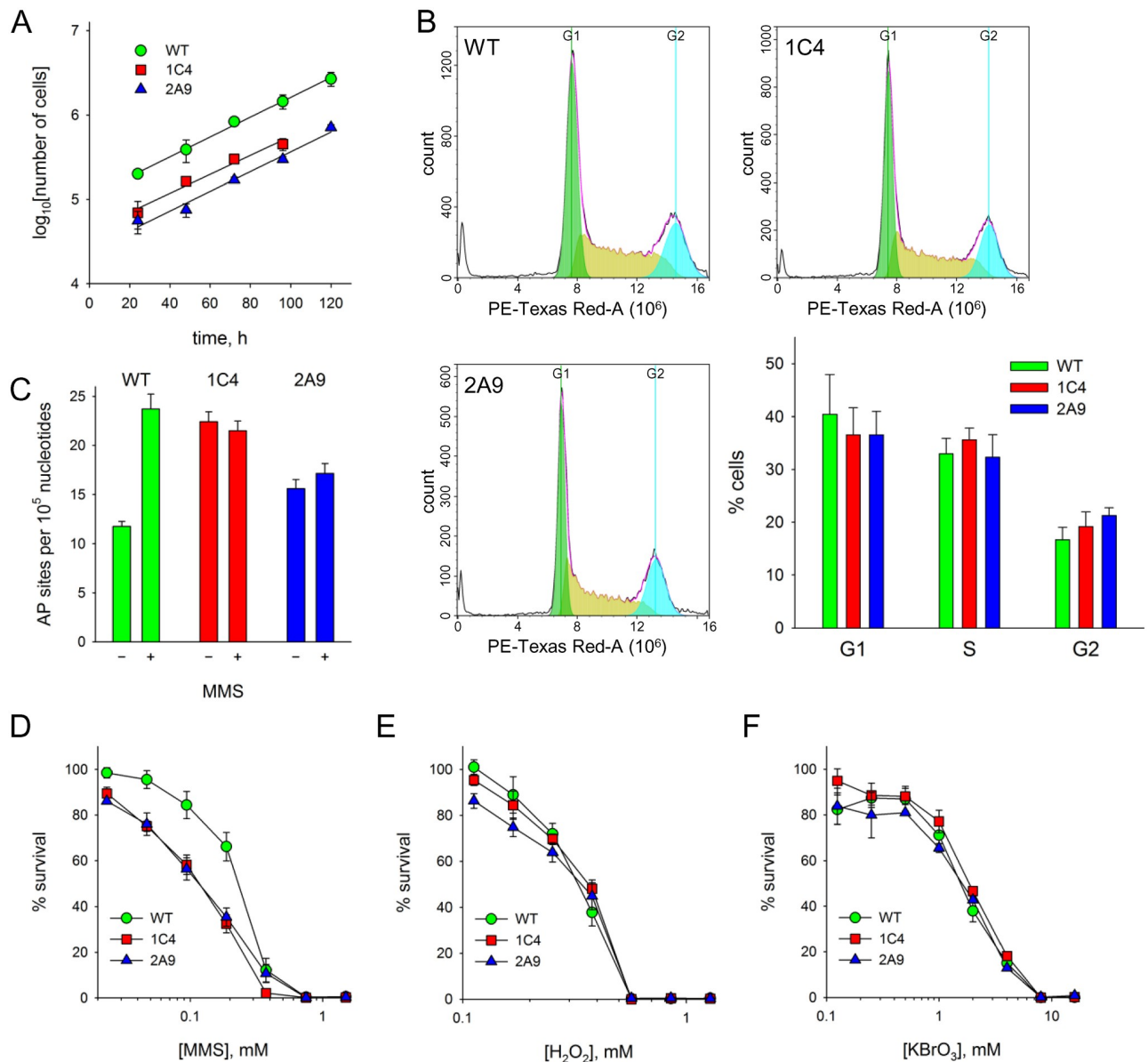
Fig 3. Phenotypic consequences of the APEX1 knockout. A, growth curves of wild-type HEK 293 (*circles*) and knockout cells 1C4 (*squares*) and 2A9 (*triangles*). Mean ± s.d. is shown (*n* = 2). **B,** cell cycle analysis of wild-type and knockout cells using propidium iodide staining. Representative cell count histograms and percentage of cells in G1, S and G2 phases in a non-synchronized population (*n* = 3, mean ± s.d.) are shown. **C,** accumulation of AP sites in wild-type HEK 293 (*green*) and knockout cells 1C4 (*red*) and 2A9 (*blue*) with and without MMS treatment. Mean ± s.d. is shown (*n* = 2). **D–F,** sensitivity of wild-type HEK 293 and knockout 1C4 and 2A9 cells to MMS (*Panel D*, *n* = 4), H_2O_2 (*Panel E*, *n* = 3) and $KBrO_3$ (*Panel F*, *n* = 3). Cell line symbols are as in *Panel A*. Mean ± s.d. is shown.

https://doi.org/10.1371/journal.pone.0257473.g003

quality control, and regulation of caspase-independent apoptosis [18, 23, 24, 59, 60]. Due to this plethora of functions and the pivotal position in the BER pathway, attempts to produce transgenic animals devoid of APEX1 have so far been unsuccessful [25–29]. Hemizygous mice are viable but demonstrate reduced BER capacity and elevated spontaneous mutagenesis [25, 27, 30, 31]. They also show perturbed vascular tone regulation due to lowered eNOS activation by SIRT1 deacetylase, which depends on the stimulation of SIRT1 by the redox function of APEX1 [61, 62]. Naturally occurring reduced-activity mutants of human APEX1 are known

[63, 64] but are exceedingly rare in the general population as germline-inherited alleles [65] so their contribution to human pathology cannot be assessed reliably.

With the advent of multiplex CRISPR/Cas9 genome editing, genome-wide knockout screens became increasingly popular to uncover the genetic basis of cell phenotypes [66]. In several recent CRISPR screens, *APEX1* knockout was shown to sensitize cells to bleomycin, temozolomide, MMS, $KBrO_3$ and illudin S (a fungal DNA-damaging sesquiterpene) [67, 68] and negatively affect cell proliferation [67, 69–72]. However, the uncovered phenotypes very much depend on the particular cell line and do not appear in many other CRISPR screens. For example, in one study only one of six patient-derived glioblastoma cell lines showed sensitivity to temozolomide upon *APEX1* knockout [67]. In the same study, the knockout affected proliferation in one of two primary neural stem cell lines and one of ten glioblastoma lines. Obviously, an *APEX1* knockout in a well-characterized cell line would be a valuable resource to study phenotypes resulting from BER inactivation.

In this study, we have knocked out the *APEX1* gene in the human HEK 293FT line and characterized the resulting cells genetically, biochemically and phenotypically. HEK 293FT is a derivative of HEK 293 line, which was long believed to originate from human embryonic kidney tissue but now, based on transcriptome profiling of several descendant lineages, is considered to come from a developing adrenal gland [73]. The group of HEK 293 descendants is surpassed only by HeLa cells in the number of research papers and only by CHO cells as a biotech production platform, and is extensively characterized at the genomic, transcriptomic and proteomic levels [73, 74]. Although HEK 293T and -FT, due to the integrated adenoviral *E1A/ E1B* genes and SV40 large T antigen expression, are more resistant to apoptosis than many other human cell lines [75, 76], they preserve intact DNA repair systems, including BER [77, 78].

We have found that the knockout cells are unable to cleave both natural and tetrahydrofuran AP sites and are deficient in BER. Although APEX1 is the major human AP endonuclease, other proteins have also been reported to cleave AP sites in human cells. APEX2, an enzyme that belongs to the same exonuclease–endonuclease–phosphatase (EEP) structural superfamily as APEX1, can hydrolyze DNA 5′ to AP sites, however, this activity is relatively weak compared with its 3′→5′-exonuclease and 3′-phosphodiesterase activities [79, 80]. The same activity was reported for aprataxin and polynucleotide kinase/3′-phosphatase like factor (APLF), a multifunctional DNA repair protein structurally unrelated to APEX1 and APEX2 [81]. Finally, many DNA glycosylases contain an AP lyase activity that efficiently cleaves DNA 3′ of aldehydic AP sites (but not THF) by β-elimination [82, 83]. However, APEX1 is a very abundant protein in human cells, including HEK 293 and its derivatives [74, 84], and all other AP endonucleases and lyases combined are evidently insufficient to support a detectable level of activity in the knockout cells.

In the absence of knockout models, most knowledge about the consequences of APEX1 functional deficiency was obtained from knockdown experiments. As with CRISPR screens mentioned above, the effects of *APEX1* downregulation are considerably cell line-dependent. It also should be kept in mind that some effects seen in APEX1-deficient cells may reflect the absence of redox or RNA-binding function of APEX1 rather than the lack of BER. Regarding HEK 293 cells and their descendants, siRNA knockdown of *APEX1* enhanced the sensitivity of HEK 293T to cisplatin and etoposide and led to a more pronounced G2/M arrest upon cisplatin treatment [85]. This, however, may not reflect BER deficiency and was attributed to a disruption of YB-1–p300 transcription regulator recruitment, which depends on APEX1 acetylation [85]. *APEX1* silencing caused an increase in apoptosis under H_2O_2 treatment [86]; however, overall cell survival was not reported in that study. In a TET1-mediated global genome

demethylation model in HEK 293T cells, *APEX1* knockdown failed to prevent clearance of 5-methylcytosine from DNA [87], suggesting the existence of some backup repair pathway for epigenetic bases oxidized by TET dioxygenases. Overall, the relatively mild phenotype in our knockout lines is consistent with the observations in HEK cells with *APEX1* downregulation. Notably, the ~2-fold increase in the background AP sites level observed in our HEK-derived cells coincides well with the results of genome-wide single-nucleotide resolution AP-specific sequencing (snAP-seq) in HeLa cells after *APEX1* knockdown, where the amount of spontaneously arising AP sites was elevated ~1.8-fold [6].

Both our knockout cell lines showed moderately lower resistance to MMS and were indistinguishable from wild-type cells in the sensitivity to H_2O_2 and $KBrO_3$. The last two agents mostly produce oxidative lesions, for which an APEX1-independent, polynucleotide kinase/3′-phosphatase (PNKP) BER branch has been described [88, 89]. In this case, BER is initiated by helix–two-turn–helix superfamily DNA glycosylases, such as NEIL1 or NEIL2, which catalyze β,δ-elimination forming a single-nucleotide gap flanked by two phosphates. PNKP further removes the 3′-phosphate generating a suitable end for a repair DNA polymerase. Also, there is growing evidence that the nucleotide excision repair pathway might contribute to oxidative damage repair in human cells [90]. H_2O_2 also yields "dirty" single-strand breaks with oxidized 3′-terminal sugar fragments that need to be removed before repair. APEX1 has this activity but human cells possess several other enzymes that can serve as 3′-repair phosphodiesterases, including APEX2, TDP1, and XPF–ERCC1 [80, 91, 92].

The case of MMS is more intriguing, as we see increased cell death but no accumulation of extra AP sites in the knockout cells. It should be emphasized that our cell survival assay employed 48 h incubation with the drug while AP site measurements were done in an acute exposure mode (1 mM MMS for 1 h), which seems to be optimal for the ARP assay [5, 93, 94]. In the pilot screening of MMS treatment conditions, concentrations >1 mM were poorly tolerated by our cells in an acute mode. The MMS exposure approximately doubled the AP sites number in wild-type cells, consistent with the literature data employing similar treatment regimens [93, 94] but had no effect on the intrinsically higher levels of ARP-detectable AP sites in the knockout cells. This lack of additional AP sites cannot be explained by the absence of excision of methylated bases by MPG, since the expression of *MPG* decreases only marginally. We hypothesize that in APEX1-deficient cells, the AP sites generated by MPG and not immediately cleaved by concerted AP endonuclease action [95] could be eventually converted to dirty strand breaks, oxidized AP sites, or DNA–protein cross-links that contribute to cell death but are hidden from ARP. Also, homologous recombination is known to contribute significantly to the prevention of MMS-induced cytotoxicity in mammalian cells [96] and could serve as a backup repair pathway in APEX1-deficient cells.

Conclusions

In summary, we have produced two APEX1 null derivatives of the commonly used HEK 293FT human non-cancer cell line and characterized them at the genetic, biochemical and phenotypic level. The knockout nature of the clones is supported by (i) lack of the wild-type allele in individually sequenced subclones; (ii) lack of protein band detectable by anti-APEX1 antibodies in the cell extracts; (iii) lack of THF- and AP site-cleaving activity in cell extracts. Despite the total abolishment of the canonical BER activity, the phenotypes of the knockout lines turned out to be relatively mild, with about a twofold increase in the background AP site levels and MMS sensitivity but nearly wild-type resistance to oxidants such as hydrogen peroxide or potassium bromate. This could indicate that mammalian cells possess mechanisms to

tolerate AP sites. Another possibility is that alternative, APEX1-independent subpathways of BER relying on bifunctional DNA glycosylases, while under the limit of detection in our experiments, might still be sufficient to keep the level of AP sites low enough for cell survival. Given the wealth of information about the parent HEK 293FT line, we hope that our knockout lines will prove useful for studies of these DNA repair pathways, their interactions, and non-repair functions of APEX1 in human cells.

Supporting information

S1 Table. Oligonucleotides used in this study.
(PDF)

S1 Fig. Sequence of the *APEX1* gene. Coding parts of the exons are highlighted green, non-coding parts of the exons are yellow. Protospacers are underlined and shown in bold. The DraIII site is boxed.
(PDF)

S2 Fig. Cleavage of the PCR-amplified part of the *APEX1* gene by DraIII. Cleavage in wild-type hypotriploid HEK293FT cells (*lanes 2*, *3*) and in wild-type nearly diploid Burkitt lymphoma BL2 cells (*lanes 4*, *5*) is shown. Arrows mark the mobility of the full-length PCR product (493 nt) and the cleavage fragments. *Lane 1*, 100-bp molecular weight markers; *lane 6*, PCR reaction with no primers.
(PDF)

S3 Fig. Sequence of the full-length APEX1 protein and its truncated variants. Sequences arising from a single-base insertion at coding position 165 (p.S56QfsX22) or a single-base deletion at coding position 165 (p.S56VfsX26) are shown. Changed polypeptide parts after the frameshift are highlighted red. The catalytic EEP domain is shown in magenta. The Cys65 residue critical for the Ref-1 activity is highlighted green.
(PDF)

S4 Fig. mRNA levels of *UNG*, *TDG*, *SMUG1*, *MBD4*, *NTHL1*, *NEIL1*, *NEIL3*, and *MPG* genes coding for various DNA glycosylases in 1C4 and 2A9 cells relative to wild-type HEK 293FT. Mean ± s.d. are shown (*n* = 2–4; see Materials and methods for a detailed description)). None of the differences between knockout and wild-type cells were statistically significant (Student's *t* rest).
(PDF)

S5 Fig. Uracil–DNA glycosylase and gap-filling activities in cell extracts. A, cleavage of a 23-mer duplex oligonucleotides containing an U:C pair by extracts of wild-type HEK293 (*lane 3*) and knockout cells 1C4 (*lane 4*) and 2A9 (*lane 5*). *Lane 1*, no enzyme or cell extract; *lane 2*, recombinant Ung. The reaction mixtures were treated with hot alkali to cleave DNA at AP sites formed by uracil removal. Arrows mark the mobility of the substrate (S) and the cleavage product (P). **B,** primer extension in a gapped substrate by extracts of wild-type HEK293 (*lanes 3–4*) and knockout cells 1C4 (*lanes 5–6*) and 2A9 (*lanes 7–8*). *Lanes 1–2*, recombinant POLβ. Arrows mark the mobility of the primer and the extension product.
(PDF)

S6 Fig. Products generated from AP site by AP endonucleases and AP lyases.
(PDF)

S7 Fig. Calibration curve of the aldehyde reactive probe assay.
(PDF)

S1 Raw images. Original images of gels and blots.
(PDF)

Acknowledgments

DNA sequencing was performed at the SB RAS Genomics Core Facility. We thank Dr. Olga Lavrik (SB RAS Institute of Chemical Biology and Fundamental Medicine, Novosibirsk, Russia) and Dr. Andriy Khobta (University of Jena, Germany) for valuable discussion.

Author Contributions

Conceptualization: Grigory L. Dianov, Dmitry O. Zharkov.

Data curation: Daria V. Kim, Vasily S. Melentyev.

Funding acquisition: Grigory L. Dianov, Dmitry O. Zharkov.

Investigation: Daria V. Kim, Liliya M. Kulishova, Natalia A. Torgasheva, Vasily S. Melentyev.

Methodology: Daria V. Kim, Vasily S. Melentyev, Sergey P. Medvedev, Suren M. Zakian, Dmitry O. Zharkov.

Project administration: Dmitry O. Zharkov.

Resources: Grigory L. Dianov, Sergey P. Medvedev, Suren M. Zakian, Dmitry O. Zharkov.

Supervision: Dmitry O. Zharkov.

Visualization: Daria V. Kim, Dmitry O. Zharkov.

Writing – original draft: Daria V. Kim, Dmitry O. Zharkov.

Writing – review & editing: Grigory L. Dianov, Suren M. Zakian, Dmitry O. Zharkov.

References

1. Lindahl T, Barnes DE. Repair of endogenous DNA damage. Cold Spring Harb Symp Quant Biol. 2000; 65:127–33. https://doi.org/10.1101/sqb.2000.65.127 PMID: 12760027

2. Friedberg EC, Walker GC, Siede W, Wood RD, Schultz RA, et al. (2006) DNA Repair and Mutagenesis. Washington, D.C.: ASM Press. 1118 p.

3. Dianov GL, Hübscher U. Mammalian base excision repair: The forgotten archangel. Nucleic Acids Res. 2013; 41:3483–90. https://doi.org/10.1093/nar/gkt076 PMID: 23408852

4. Lindahl T, Nyberg B. Rate of depurination of native deoxyribonucleic acid. Biochemistry. 1972; 11:3610–8. https://doi.org/10.1021/bi00769a018 PMID: 4626532

5. Atamna H, Cheung I, Ames BN. A method for detecting abasic sites in living cells: Age-dependent changes in base excision repair. Proc Natl Acad Sci USA. 2000; 97:686–91. https://doi.org/10.1073/pnas.97.2.686 PMID: 10639140

6. Liu ZJ, Martínez Cuesta S, van Delft P, Balasubramanian S. Sequencing abasic sites in DNA at single-nucleotide resolution. Nat Chem. 2019; 11:629–37. https://doi.org/10.1038/s41557-019-0279-9 PMID: 31209299

7. Strauss BS. The "A" rule revisited: Polymerases as determinants of mutational specificity. DNA Repair. 2002; 1:125–35. https://doi.org/10.1016/s1568-7864(01)00014-3 PMID: 12509259

8. Taylor J-S. New structural and mechanistic insight into the A-rule and the instructional and non-instructional behavior of DNA photoproducts and other lesions. Mutat Res. 2002; 510:55–70. https://doi.org/10.1016/s0027-5107(02)00252-x PMID: 12459443

9. Pourquier P, Ueng L-M, Kohlhagen G, Mazumder A, Gupta M, et al. Effects of uracil incorporation, DNA mismatches, and abasic sites on cleavage and religation activities of mammalian topoisomerase I. J Biol Chem. 1997; 272:7792–6. https://doi.org/10.1074/jbc.272.12.7792 PMID: 9065442

10. Doetsch PW. Translesion synthesis by RNA polymerases: Occurrence and biological implications for transcriptional mutagenesis. Mutat Res. 2002; 510:131–40. https://doi.org/10.1016/s0027-5107(02)00258-0 PMID: 12459449

11. Quiñones JL, Demple B. When DNA repair goes wrong: BER-generated DNA-protein crosslinks to oxidative lesions. DNA Repair. 2016; 44:103–9. https://doi.org/10.1016/j.dnarep.2016.05.014 PMID: 27264558

12. Rahimoff R, Kosmatchev O, Kirchner A, Pfaffeneder T, Spada F, et al. 5-Formyl- and 5-carboxydeoxy-cytidines do not cause accumulation of harmful repair intermediates in stem cells. J Am Chem Soc. 2017; 139:10359–64. https://doi.org/10.1021/jacs.7b04131 PMID: 28715893

13. Guillet M, Boiteux S. Endogenous DNA abasic sites cause cell death in the absence of Apn1, Apn2 and Rad1/Rad10 in *Saccharomyces cerevisiae*. EMBO J. 2002; 21:2833–41. https://doi.org/10.1093/emboj/21.11.2833 PMID: 12032096

14. Cunningham RP, Saporito SM, Spitzer SG, Weiss B. Endonuclease IV (*nfo*) mutant of *Escherichia coli*. J Bacteriol. 1986; 168:1120–7. https://doi.org/10.1128/jb.168.3.1120-1127.1986 PMID: 2430946

15. Foster PL. *Escherichia coli* strains with multiple DNA repair defects are hyperinduced for the SOS response. J Bacteriol. 1990; 172:4719–20. https://doi.org/10.1128/jb.172.8.4719-4720.1990 PMID: 2115878

16. Janion C, Sikora A, Nowosielska A, Grzesiuk E. *E. coli* BW535, a triple mutant for the DNA repair genes *xth*, *nth*, and *nfo*, chronically induces the SOS response. Environ Mol Mutagen. 2003; 41:237–42. https://doi.org/10.1002/em.10154 PMID: 12717778

17. Demple B, Sung J-S. Molecular and biological roles of Ape1 protein in mammalian base excision repair. DNA Repair. 2005; 4:1442–9. https://doi.org/10.1016/j.dnarep.2005.09.004 PMID: 16199212

18. Tell G, Quadrifoglio F, Tiribelli C, Kelley MR. The many functions of APE1/Ref-1: Not only a DNA repair enzyme. Antioxid Redox Signal. 2009; 11:601–20. https://doi.org/10.1089/ars.2008.2194 PMID: 18976116

19. Tell G, Fantini D, Quadrifoglio F. Understanding different functions of mammalian AP endonuclease (APE1) as a promising tool for cancer treatment. Cell Mol Life Sci. 2010; 67:3589–608. https://doi.org/10.1007/s00018-010-0486-4 PMID: 20706766

20. McNeill DR, Whitaker AM, Stark WJ, Illuzzi JL, McKinnon PJ, et al. Functions of the major abasic endonuclease (APE1) in cell viability and genotoxin resistance. Mutagenesis. 2020; 35:27–38. https://doi.org/10.1093/mutage/gez046 PMID: 31816044

21. Xanthoudakis S, Miao G, Wang F, Pan Y-CE, Curran T. Redox activation of Fos–Jun DNA binding activity is mediated by a DNA repair enzyme. EMBO J. 1992; 11:3323–35. https://doi.org/10.1002/j.1460-2075.1992.tb05411.x PMID: 1380454

22. Xanthoudakis S, Miao GG, Curran T. The redox and DNA-repair activities of Ref-1 are encoded by non-overlapping domains. Proc Natl Acad Sci USA. 1994; 91:23–7. https://doi.org/10.1073/pnas.91.1.23 PMID: 7506414

23. Antoniali G, Malfatti MC, Tell G. Unveiling the non-repair face of the Base Excision Repair pathway in RNA processing: A missing link between DNA repair and gene expression? DNA Repair. 2017; 56:65–74. https://doi.org/10.1016/j.dnarep.2017.06.008 PMID: 28629776

24. Malfatti MC, Antoniali G, Codrich M, Burra S, Mangiapane G, et al. New perspectives in cancer biology from a study of canonical and non-canonical functions of base excision repair proteins with a focus on early steps. Mutagenesis. 2020; 35:129–49. https://doi.org/10.1093/mutage/gez051 PMID: 31858150

25. Xanthoudakis S, Smeyne RJ, Wallace JD, Curran T. The redox/DNA repair protein, Ref-1, is essential for early embryonic development in mice. Proc Natl Acad Sci USA. 1996; 93:8919–23. https://doi.org/10.1073/pnas.93.17.8919 PMID: 8799128

26. Ludwig DL, MacInnes MA, Takiguchi Y, Purtymun PE, Henrie M, et al. A murine AP-endonuclease gene-targeted deficiency with post-implantation embryonic progression and ionizing radiation sensitivity. Mutat Res. 1998; 409:17–29. https://doi.org/10.1016/s0921-8777(98)00039-1 PMID: 9806499

27. Meira LB, Devaraj S, Kisby GE, Burns DK, Daniel RL, et al. Heterozygosity for the mouse *Apex* gene results in phenotypes associated with oxidative stress. Cancer Res. 2001; 61:5552–7. PMID: 11454706

28. Izumi T, Brown DB, Naidu CV, Bhakat KK, MacInnes MA, et al. Two essential but distinct functions of the mammalian abasic endonuclease. Proc Natl Acad Sci USA. 2005; 102:5739–43. https://doi.org/10.1073/pnas.0500986102 PMID: 15824325

29. Wang Y, Shupenko CC, Melo LF, Strauss PR. DNA repair protein involved in heart and blood development. Mol Cell Biol. 2006; 26:9083–93. https://doi.org/10.1128/MCB.01216-06 PMID: 16966376

30. Huamani J, McMahan CA, Herbert DC, Reddick R, McCarrey JR, et al. Spontaneous mutagenesis is enhanced in *Apex* heterozygous mice. Mol Cell Biol. 2004; 24:8145–53. https://doi.org/10.1128/MCB.24.18.8145-8153.2004 PMID: 15340075

31. Raffoul JJ, Cabelof DC, Nakamura J, Meira LB, Friedberg EC, et al. Apurinic/apyrimidinic endonuclease (APE/REF-1) haploinsufficient mice display tissue-specific differences in DNA polymerase β-dependent base excision repair. J Biol Chem. 2004; 279:18425–33. https://doi.org/10.1074/jbc.M313983200 PMID: 14973123

32. Kim DV, Makarova AV, Miftakhova RR, Zharkov DO. Base excision DNA repair deficient cells: From disease models to genotoxicity sensors. Curr Pharm Des. 2019; 25:298–312. https://doi.org/10.2174/1381612825666190319112930 PMID: 31198112

33. Masani S, Han L, Yu K. Apurinic/apyrimidinic endonuclease 1 is the essential nuclease during immuno-globulin class switch recombination. Mol Cell Biol. 2013; 33:1468–73. https://doi.org/10.1128/MCB.00026-13 PMID: 23382073

34. Chen T, Liu C, Lu H, Yin M, Shao C, et al. The expression of APE1 in triple-negative breast cancer and its effect on drug sensitivity of olaparib. Tumor Biol. 2017; 39:1010428317713390. https://doi.org/10.1177/1010428317713390 PMID: 29064327

35. Walker LJ, Craig RB, Harris AL, Hickson ID. A role for the human DNA repair enzyme HAP1 in cellular protection against DNA damaging agents and hypoxic stress. Nucleic Acids Res. 1994; 22:4884–9. https://doi.org/10.1093/nar/22.23.4884 PMID: 7800476

36. Silber JR, Bobola MS, Blank A, Schoeler KD, Haroldson PD, et al. The apurinic/apyrimidinic endonucle-ase activity of Ape1/Ref-1 contributes to human glioma cell resistance to alkylating agents and is ele-vated by oxidative stress. Clin Cancer Res. 2002; 8:3008–18. PMID: 12231548

37. Wang D, Luo M, Kelley MR. Human apurinic endonuclease 1 (APE1) expression and prognostic signifi-cance in osteosarcoma: Enhanced sensitivity of osteosarcoma to DNA damaging agents using silenc-ing RNA APE1 expression inhibition. Mol Cancer Ther. 2004; 3:679–86. PMID: 15210853

38. Fung H, Demple B. Distinct roles of Ape1 protein in the repair of DNA damage induced by ionizing radia-tion or bleomycin. J Biol Chem. 2011; 286:4968–77. https://doi.org/10.1074/jbc.M110.146498 PMID: 21081487

39. Ran FA, Hsu PD, Wright J, Agarwala V, Scott DA, et al. Genome engineering using the CRISPR-Cas9 system. Nat Protoc. 2013; 8:2281–308. https://doi.org/10.1038/nprot.2013.143 PMID: 24157548

40. Sidorenko VS, Nevinsky GA, Zharkov DO. Mechanism of interaction between human 8-oxoguanine-DNA glycosylase and AP endonuclease. DNA Repair. 2007; 6:317–28. https://doi.org/10.1016/j.dnarep.2006.10.022 PMID: 17126083

41. Kumar A, Widen SG, Williams KR, Kedar P, Karpel RL, et al. Studies of the domain structure of mam-malian DNA polymerase β: Identification of a discrete template binding domain. J Biol Chem. 1990; 265:2124–31. https://doi.org/10.1016/S0021-9258(19)39949-1 PMID: 2404980

42. Matsuzaki Y, Umemoto T, Tanaka Y, Okano T, Yamato M. β2-Microglobulin is an appropriate reference gene for RT-PCR-based gene expression analysis of hematopoietic stem cells. Regen Ther. 2015; 1:91–7. https://doi.org/10.1016/j.reth.2015.04.003 PMID: 31245448

43. Sobol RW, Prasad R, Evenski A, Baker A, Yang X-P, et al. The lyase activity of the DNA repair protein β-polymerase protects from DNA-damage-induced cytotoxicity. Nature. 2000; 405:807–10. https://doi.org/10.1038/35015598 PMID: 10866204

44. Hsu PD, Scott DA, Weinstein JA, Ran FA, Konermann S, et al. DNA targeting specificity of RNA-guided Cas9 nucleases. Nat Biotechnol. 2013; 31:827–32. https://doi.org/10.1038/nbt.2647 PMID: 23873081

45. Doench JG, Fusi N, Sullender M, Hegde M, Vaimberg EW, et al. Optimized sgRNA design to maximize activity and minimize off-target effects of CRISPR-Cas9. Nat Biotechnol. 2016; 34:184–91. https://doi.org/10.1038/nbt.3437 PMID: 26780180

46. Brinkman EK, Chen T, Amendola M, van Steensel B. Easy quantitative assessment of genome editing by sequence trace decomposition. Nucleic Acids Res. 2014; 42:e168. https://doi.org/10.1093/nar/gku936 PMID: 25300484

47. Miller H, Prasad R, Wilson SH, Johnson F, Grollman AP. 8-OxodGTP incorporation by DNA polymerase β is modified by active-site residue Asn279. Biochemistry. 2000; 39:1029–33. https://doi.org/10.1021/bi991789x PMID: 10653647

48. Kubo K, Ide H, Wallace SS, Kow YW. A novel sensitive and specific assay for abasic sites, the most commonly produced DNA lesion. Biochemistry. 1992; 31:3703–8. https://doi.org/10.1021/bi00129a020 PMID: 1567824

49. Wyatt MD, Pittman DL. Methylating agents and DNA repair responses: Methylated bases and sources of strand breaks. Chem Res Toxicol. 2006; 19:1580–94. https://doi.org/10.1021/tx060164e PMID: 17173371

50. Greenberg MM. Abasic and oxidized abasic site reactivity in DNA: Enzyme inhibition, cross-linking, and nucleosome catalyzed reactions. Acc Chem Res. 2014; 47:646–55. https://doi.org/10.1021/ar400229d PMID: 24369694

51. Pachva MC, Kisselev AF, Matkarimov BT, Saparbaev M, Groisman R. DNA-histone cross-links: Formation and repair. Front Cell Dev Biol. 2020; 8:607045. https://doi.org/10.3389/fcell.2020.607045 PMID: 33409281

52. Blakely WF, Fuciarelli AF, Wegher BJ, Dizdaroglu M. Hydrogen peroxide-induced base damage in deoxyribonucleic acid. Radiat Res. 1990; 121:338–43. PMID: 2315450

53. Pogozelski WK, Tullius TD. Oxidative strand scission of nucleic acids: Routes initiated by hydrogen abstraction from the sugar moiety. Chem Rev. 1998; 98:1089–107. https://doi.org/10.1021/cr960437i PMID: 11848926

54. Parsons JL, Chipman JK. The role of glutathione in DNA damage by potassium bromate *in vitro*. Mutagenesis. 2000; 15:311–6. https://doi.org/10.1093/mutage/15.4.311 PMID: 10887209

55. Ballmaier D, Epe B. DNA damage by bromate: Mechanism and consequences. Toxicology. 2006; 221:166–71. https://doi.org/10.1016/j.tox.2006.01.009 PMID: 16490296

56. Beranek DT. Distribution of methyl and ethyl adducts following alkylation with monofunctional alkylating agents. Mutat Res. 1990; 231:11–30. https://doi.org/10.1016/0027-5107(90)90173-2 PMID: 2195323

57. Engelward BP, Dreslin A, Christensen J, Huszar D, Kurahara C, et al. Repair-deficient 3-methyladenine DNA glycosylase homozygous mutant mouse cells have increased sensitivity to alkylation-induced chromosome damage and cell killing. EMBO J. 1996; 15:945–52. https://doi.org/10.1002/j.1460-2075.1996.tb00429.x PMID: 8631315

58. Roth RB, Samson LD. 3-Methyladenine DNA glycosylase-deficient *Aag* null mice display unexpected bone marrow alkylation resistance. Cancer Res. 2002; 62:656–60. PMID: 11830515

59. Fan Z, Beresford PJ, Zhang D, Xu Z, Novina CD, et al. Cleaving the oxidative repair protein Ape1 enhances cell death mediated by granzyme A. Nat Immunol. 2003; 4:145–53. https://doi.org/10.1038/ni885 PMID: 12524539

60. Popov AV, Grin IR, Dvornikova AP, Matkarimov BT, Groisman R, et al. Reading targeted DNA damage in the active demethylation pathway: Role of accessory domains of eukaryotic AP endonucleases and thymine-DNA glycosylases. J Mol Biol. 2020; 432:1747–68. https://doi.org/10.1016/j.jmb.2019.12.020 PMID: 31866293

61. Jeon BH, Gupta G, Park YC, Qi B, Haile A, et al. Apurinic/apyrimidinic endonuclease 1 regulates endothelial NO production and vascular tone. Circ Res. 2004; 95:902–10. https://doi.org/10.1161/01.RES.0000146947.84294.4c PMID: 15472121

62. Jung S-B, Kim C-S, Kim Y-R, Naqvi A, Yamamori T, et al. Redox factor-1 activates endothelial SIRTUIN1 through reduction of conserved cysteine sulfhydryls in its deacetylase domain. PLoS ONE. 2013; 8:e65415. https://doi.org/10.1371/journal.pone.0065415 PMID: 23755229

63. Hadi MZ, Coleman MA, Fidelis K, Mohrenweiser HW, Wilson DM, III. Functional characterization of Ape1 variants identified in the human population. Nucleic Acids Res. 2000; 28:3871–9. https://doi.org/10.1093/nar/28.20.3871 PMID: 11024165

64. Illuzzi JL, Harris NA, Manvilla BA, Kim D, Li M, et al. Functional assessment of population and tumor-associated APE1 protein variants. PLoS ONE. 2013; 8:e65922. https://doi.org/10.1371/journal.pone.0065922 PMID: 23776569

65. Karczewski KJ, Francioli LC, Tiao G, Cummings BB, Alföldi J, et al. The mutational constraint spectrum quantified from variation in 141,456 humans. Nature. 2020; 581:434–43. https://doi.org/10.1038/s41586-020-2308-7 PMID: 32461654

66. Shalem O, Sanjana NE, Zhang F. High-throughput functional genomics using CRISPR–Cas9. Nat Rev Genet. 2015; 16:299–311. https://doi.org/10.1038/nrg3899 PMID: 25854182

67. MacLeod G, Bozek DA, Rajakulendran N, Monteiro V, Ahmadi M, et al. Genome-wide CRISPR-Cas9 screens expose genetic vulnerabilities and mechanisms of temozolomide sensitivity in glioblastoma stem cells. Cell Rep. 2019; 27:971–86.e9. https://doi.org/10.1016/j.celrep.2019.03.047 PMID: 30995489

68. Olivieri M, Cho T, Álvarez-Quilón A, Li K, Schellenberg MJ, et al. A genetic map of the response to DNA damage in human cells. Cell. 2020; 182:481–96.e21. https://doi.org/10.1016/j.cell.2020.05.040 PMID: 32649862

69. Toledo CM, Ding Y, Hoellerbauer P, Davis RJ, Basom R, et al. Genome-wide CRISPR-Cas9 screens reveal loss of redundancy between PKMYT1 and WEE1 in glioblastoma stem-like cells. Cell Rep. 2015; 13:2425–39. https://doi.org/10.1016/j.celrep.2015.11.021 PMID: 26673326

70. Aguirre AJ, Meyers RM, Weir BA, Vazquez F, Zhang C-Z, et al. Genomic copy number dictates a gene-independent cell response to CRISPR/Cas9 targeting. Cancer Discov. 2016; 6:914–29. https://doi.org/10.1158/2159-8290.CD-16-0154 PMID: 27260156

71. Behan FM, Iorio F, Picco G, Gonçalves E, Beaver CM, et al. Prioritization of cancer therapeutic targets using CRISPR–Cas9 screens. Nature. 2019; 568:511–6. https://doi.org/10.1038/s41586-019-1103-9 PMID: 30971826

72. Liang J, Zhao H, Diplas BH, Liu S, Liu J, et al. Genome-wide CRISPR-Cas9 screen reveals selective vulnerability of ATRX-mutant cancers to WEE1 inhibition. Cancer Res. 2020; 80:510–23. https://doi.org/10.1158/0008-5472.CAN-18-3374 PMID: 31551363

73. Lin Y-C, Boone M, Meuris L, Lemmens I, Van Roy N, et al. Genome dynamics of the human embryonic kidney 293 lineage in response to cell biology manipulations. Nat Commun. 2014; 5:4767. https://doi.org/10.1038/ncomms5767 PMID: 25182477

74. Geiger T, Wehner A, Schaab C, Cox J, Mann M. Comparative proteomic analysis of eleven common cell lines reveals ubiquitous but varying expression of most proteins. Mol Cell Proteomics. 2012; 11: M111.014050. https://doi.org/10.1074/mcp.M111.014050 PMID: 22278370

75. Ahuja D, Sáenz-Robles MT, Pipas JM. SV40 large T antigen targets multiple cellular pathways to elicit cellular transformation. Oncogene. 2005; 24:7729–45. https://doi.org/10.1038/sj.onc.1209046 PMID: 16299533

76. Berk AJ. Recent lessons in gene expression, cell cycle control, and cell biology from adenovirus. Oncogene. 2005; 24:7673–85. https://doi.org/10.1038/sj.onc.1209040 PMID: 16299528

77. Shen J-C, Fox EJ, Ahn EH, Loeb LA. A rapid assay for measuring nucleotide excision repair by oligonucleotide retrieval. Sci Rep. 2014; 4:4894. https://doi.org/10.1038/srep04894 PMID: 24809800

78. Golato T, Brenerman B, McNeill DR, Li J, Sobol RW, et al. Development of a cell-based assay for measuring base excision repair responses. Sci Rep. 2017; 7:13007. https://doi.org/10.1038/s41598-017-12963-7 PMID: 29021553

79. Hadi MZ, Ginalski K, Nguyen LH, Wilson DM, III. Determinants in nuclease specificity of Ape1 and Ape2, human homologues of *Escherichia coli* exonuclease III. J Mol Biol. 2002; 316:853–66. https://doi.org/10.1006/jmbi.2001.5382 PMID: 11866537

80. Burkovics P, Szukacsov V, Unk I, Haracska L. Human Ape2 protein has a 3′–5′ exonuclease activity that acts preferentially on mismatched base pairs. Nucleic Acids Res. 2006; 34:2508–15. https://doi.org/10.1093/nar/gkl259 PMID: 16687656

81. Kanno S-i, Kuzuoka H, Sasao S, Hong Z, Lan L, et al. A novel human AP endonuclease with conserved zinc-finger-like motifs involved in DNA strand break responses. EMBO J. 2007; 26:2094–103. https://doi.org/10.1038/sj.emboj.7601663 PMID: 17396150

82. McCullough AK, Dodson ML, Lloyd RS. Initiation of base excision repair: Glycosylase mechanisms and structures. Annu Rev Biochem. 1999; 68:255–85. https://doi.org/10.1146/annurev.biochem.68.1.255 PMID: 10872450

83. McCullough AK, Sanchez A, Dodson ML, Marapaka P, Taylor J-S, et al. The reaction mechanism of DNA glycosylase/AP lyases at abasic sites. Biochemistry. 2001; 40:561–8. https://doi.org/10.1021/bi002404+ PMID: 11148051

84. Wang M, Herrmann CJ, Simonovic M, Szklarczyk D, von Mering C. Version 4.0 of PaxDb: Protein abundance data, integrated across model organisms, tissues, and cell-lines. Proteomics. 2015; 15:3163–8. https://doi.org/10.1002/pmic.201400441 PMID: 25656970

85. Sengupta S, Mantha AK, Mitra S, Bhakat KK. Human AP endonuclease (APE1/Ref-1) and its acetylation regulate YB-1-p300 recruitment and RNA polymerase II loading in the drug-induced activation of multidrug resistance gene *MDR1*. Oncogene. 2011; 30:482–93. https://doi.org/10.1038/onc.2010.435 PMID: 20856196

86. Xiong J-J, Zhang Y, Wang J-L, Bao G-D, Zhang Y, et al. Silencing of Ref-1 expression by retrovirus-mediated shRNA sensitizes HEK293 cells to hydrogen peroxide-induced apoptosis. Biosci Biotechnol Biochem. 2008; 72:3206–10. https://doi.org/10.1271/bbb.80415 PMID: 19060414

87. Jin C, Qin T, Barton MC, Jelinek J, Issa J-PJ. Minimal role of base excision repair in TET-induced global DNA demethylation in HEK293T cells. Epigenetics. 2015; 10:1006–13. https://doi.org/10.1080/15592294.2015.1091145 PMID: 26440216

88. Wiederhold L, Leppard JB, Kedar P, Karimi-Busheri F, Rasouli-Nia A, et al. AP endonuclease-independent DNA base excision repair in human cells. Mol Cell. 2004; 15:209–20. https://doi.org/10.1016/j.molcel.2004.06.003 PMID: 15260972

89. Das A, Wiederhold L, Leppard JB, Kedar P, Prasad R, et al. NEIL2-initiated, APE-independent repair of oxidized bases in DNA: Evidence for a repair complex in human cells. DNA Repair. 2006; 5:1439–48. https://doi.org/10.1016/j.dnarep.2006.07.003 PMID: 16982218

90. Shafirovich V, Geacintov NE. Removal of oxidatively generated DNA damage by overlapping repair pathways. Free Radic Biol Med. 2017; 107:53–61. https://doi.org/10.1016/j.freeradbiomed.2016.10.507 PMID: 27818219

91. Pommier Y, Huang S-yN, Gao R, Das BB, Murai J, et al. Tyrosyl-DNA-phosphodiesterases (TDP1 and TDP2). DNA Repair. 2014; 19:114–29. https://doi.org/10.1016/j.dnarep.2014.03.020 PMID: 24856239

92. Fisher LA, Samson L, Bessho T. Removal of reactive oxygen species-induced 3′-blocked ends by XPF-ERCC1. Chem Res Toxicol. 2011; 24:1876–81. https://doi.org/10.1021/tx200221j PMID: 22007867

93. Asaeda A, Ide H, Tano K, Takamori Y, Kubo K. Repair kinetics of abasic sites in mammalian cells selectively monitored by the aldehyde reactive probe (ARP). Nucleosides Nucleotides. 1998; 17:503–13. https://doi.org/10.1080/07328319808005194 PMID: 9708359

94. Condie AG, Yan Y, Gerson SL, Wang Y. A fluorescent probe to measure DNA damage and repair. PLoS ONE. 2015; 10:e0131330. https://doi.org/10.1371/journal.pone.0131330 PMID: 26309022

95. Xia L, Zheng L, Lee H-W, Bates SE, Federico L, et al. Human 3-methyladenine-DNA glycosylase: Effect of sequence context on excision, association with PCNA, and stimulation by AP endonuclease. J Mol Biol. 2005; 346:1259–74. https://doi.org/10.1016/j.jmb.2005.01.014 PMID: 15713479

96. Nikolova T, Ensminger M, Löbrich M, Kaina B. Homologous recombination protects mammalian cells from replication-associated DNA double-strand breaks arising in response to methyl methanesulfonate. DNA Repair. 2010; 9:1050–63. https://doi.org/10.1016/j.dnarep.2010.07.005 PMID: 20708982